J|A|C|S ARTICLES

Published on Web 04/02/2009

Mechanistic Insights into Catalytic H_2 Oxidation by Ni Complexes Containing a Diphosphine Ligand with a Positioned Amine Base

Jenny Y. Yang, R. Morris Bullock, Wendy J. Shaw, Brendan Twamley,[†] Kendra Fraze,[‡] M. Rakowski DuBois, and Daniel L. DuBois*

Chemical and Materials Sciences Division, Pacific Northwest National Laboratory, Richland, Washington 99352

Received January 23, 2009; E-mail: daniel.dubois@pnl.gov

Abstract: The mixed-ligand complex [Ni(dppp)($P^{Ph}_2N^{Bz}_2$)](BF_4)$_2$, **3**, (where $P^{Ph}_2N^{Bz}_2$ is 1,5-dibenzyl-3,7-diphenyl-1,5-diaza-3,7-diphosphacyclooctane and dppp is 1,3-bis(diphenylphosphino)propane) has been synthesized. Treatment of this complex with H_2 and triethylamine results in the formation of the Ni^0 complex, Ni(dppp)($P^{Ph}_2N^{Bz}_2$), **4**, whose structure has been determined by a single-crystal X-ray diffraction study. Heterolytic cleavage of H_2 by **3** at room temperature forms [HNi(dppp)($P^{Ph}_2N^{Bz}$(μ-H)N^{Bz})](BF_4)$_2$, **5a**, in which one proton interacts with two nitrogen atoms of the cyclic diphosphine ligand and a hydride ligand is bound to nickel. Two intermediates are observed for this reaction using low-temperature NMR spectroscopy. One species is a dihydride, [$(H)_2$Ni(dppp)($P^{Ph}_2N^{Bz}_2$)](BF_4)$_2$, **5b**, and the other is [Ni(dppp)($P^{Ph}_2N^{Bz}_2H_2$)](BF_4)$_2$, **5c**, in which both protons are bound to the N atoms in an endo geometry with respect to nickel. These two species interconvert via a rapid and reversible intramolecular proton exchange between nickel and the nitrogen atoms of the diphosphine ligand. Complex **3** is a catalyst for the electrochemical oxidation of H_2 in the presence of base, and new insights into the mechanism derived from low-temperature NMR and thermodynamic studies are presented. A comparison of the rate and thermodynamics of H_2 addition for this complex to related catalysts studied previously indicates that for Ni^{II} complexes containing two diphosphine ligands, the activation of H_2 is favored by the presence of *two positioned* pendant bases.

Introduction

The potential use of hydrogen in future energy storage and delivery systems based on renewable energy sources has spurred interest in many aspects of hydrogen production, storage, and utilization, as indicated by a number of recent thematic issues on this subject.[1−3] Of particular interest for the production and utilization of hydrogen is the development of new electrocatalysts that are not based on platinum. Current polymer electrolyte membrane (PEM) fuel cells use platinum as the catalyst for both half-reactions, oxidation of hydrogen and reduction of oxygen. A major drawback, however, is that platinum is expensive. Structural studies of hydrogenase enzymes have clearly demonstrated that abundant, inexpensive metals such as nickel and iron are capable of catalyzing the efficient oxidation and production of hydrogen.[4−8] This has led to a number of studies to mimic the structure and function of these enzymes with small molecular complexes[2,3,9−12] and to the development of synthetic catalysts that are functional but not structural mimics of the enzymes.[13−17]

We recently reported the syntheses and studies of nickel,[18−22] iron,[23−26] and cobalt[27] diphosphine complexes with noncoor-

[†] Department of Chemistry, University of Idaho, Moscow, ID 83844.
[‡] Department of Chemistry and Biochemistry, University of Colorado, Boulder, CO 80309.

(1) Lubitz, W.; Tumas, W. *Chem. Rev.* **2007**, *107*, 3899–4436.
(2) Schollhammer, P.; Talarmin, J. *C. R. Chim.* **2008**, *11*, 789–944.
(3) Pickett, C. J.; Best, S. P. *Coord. Chem. Rev.* **2005**, *249*, 1517–1690.
(4) Frey, M. *ChemBioChem* **2002**, *3*, 153–160.
(5) Peters, J. W. *Curr. Opin. Struct. Biol.* **1999**, *9*, 670–676.
(6) Peters, J. W.; Lanzilotta, W. N.; Lemon, B. J.; Seefeldt, L. C. *Science* **1998**, *282*, 1853–1858.
(7) Nicolet, Y.; de Lacey, A. L.; Vernède, X.; Fernandez, V. M.; Hatchikian, E. C.; Fontecilla-Camps, J. C. *J. Am. Chem. Soc.* **2001**, *123*, 1596–1601.
(8) Fontecilla-Camps, J. C.; Volbeda, A.; Cavazza, C.; Nicolet, Y. *Chem. Rev.* **2007**, *107*, 4273–4303.
(9) (a) Barton, B. E.; Olsen, M. T.; Rauchfuss, T. B. *J. Am. Chem. Soc.* **2008**, *130*, 16834–16835. (b) Gloaguen, F.; Rauchfuss, T. B. *Chem. Soc. Rev.* **2009**, *38*, 100–108.
(10) Liu, T.; Darensbourg, M. Y. *J. Am. Chem. Soc.* **2007**, *129*, 7008–7009.
(11) Löscher, S.; Schwartz, L.; Stein, M.; Ott, S.; Haumann, M. *Inorg. Chem.* **2007**, *46*, 11094–11105.
(12) Artero, V.; Fontecave, M. *Coord. Chem. Rev.* **2005**, *249*, 1518–1535.
(13) Hu, X.; Brunschwig, B. S.; Peters, J. C. *J. Am. Chem. Soc.* **2007**, *129*, 8988–8998.
(14) Hu, X. L.; Cossairt, B. M.; Brunschwig, B. S.; Lewis, N. S.; Peters, J. C. *Chem. Commun.* **2005**, 4723–4725.
(15) Connolly, P.; Espenson, J. H. *Inorg. Chem.* **1986**, *25*, 2684–2688.
(16) Baffert, C.; Artero, V.; Fontecave, M. *Inorg. Chem.* **2007**, *46*, 1817–1824.
(17) Appel, A. M.; DuBois, D. L.; DuBois, M. R. *J. Am. Chem. Soc.* **2005**, *127*, 12717–12726.
(18) Curtis, C. J.; Miedaner, A.; Ciancanelli, R. F.; Ellis, W. W.; Noll, B. C.; Rakowski DuBois, M.; DuBois, D. L. *Inorg. Chem.* **2003**, *42*, 216–227.
(19) Wilson, A. D.; Newell, R. H.; McNevin, M. J.; Muckerman, J. T.; Rakowski DuBois, M.; DuBois, D. L. *J. Am. Chem. Soc.* **2006**, *128*, 358–366.
(20) Wilson, A. D.; Miedaner, A.; Muckerman, J. T.; DuBois, D. L.; Rakowski DuBois, M. *Proc. Nat. Acad. Sci U.S.A.* **2007**, *104*, 6951–6956.

dinating pendant amine bases incorporated into the backbone of the ligands. The pendant bases in these complexes perform a number of functions that are potentially important in the catalytic oxidation or formation of hydrogen, as well as other processes that require multiple electron/proton transfers. Their roles in these synthetic complexes have included stabilizing the binding of H_2 to the metal center, assisting the heterolytic cleavage of coordinated dihydrogen, facilitating intra- and intermolecular proton transfer, and coupling proton and electron transfer events.[28,29] As a result, nickel and cobalt complexes containing diphosphine ligands with amine bases (or proton relays) in the second coordination sphere exhibit much higher catalytic rates and lower overpotentials for H_2 production and oxidation than analogous compounds lacking these relays.

For example, the complexes $[Ni(P^{Ph}_2N^{Ph}_2)_2(CH_3CN)](BF_4)_2$ and $[Ni(P^{Cy}_2N^{Bz}_2)_2](BF_4)_2$ each contain two amine bases positioned within 3.4 Å of the nickel ion, and the complexes serve as effective electrocatalysts for the formation and oxidation of hydrogen, respectively. In the reaction of hydrogen with $[Ni(P^{Cy}_2N^{Bz}_2)_2](BF_4)_2$, the first product observed in low-temperature NMR spectroscopic studies is a reduced Ni^0 product in which a pendant amine in each of the ligands is protonated. The nature of the product suggests that the interaction of *two* positioned pendant bases with the incoming H_2 molecule helps stabilize its addition to the nickel ion, as shown in **1**,[20,21] and we postulated that this interaction is necessary for the relatively high rate of H_2 oxidation observed for this catalyst. More recently, however, we found that $[Co(CH_3CN)_3(P^{Ph}_2N^{Ph}_2)](BF_4)_2$, **2**, which contains only one positioned proton relay, shows high rates for the electrocatalytic formation of H_2.[27]

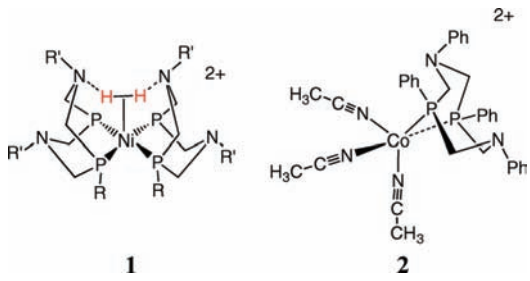

1 **2**

As part of our efforts in catalyst design, we wished to further investigate how the number of positioned proton relays influences the catalytic rates of these nickel complexes. We have therefore synthesized the new mixed-ligand complexes in which a single amine base is positioned near the nickel ion, $[Ni(dppp)(N^{Ph}_2P^{Bz}_2)](BF_4)_2$, **3**, and $[Ni(dppp)(N^{Ph}_2P^{Bz}_2)]$, **4**. The reactions of the Ni(II) complex with H_2, and of the Ni^0 complex with protons have been monitored by multinuclear NMR spectroscopy at low temperatures, and a rate for electrocatalytic H_2 oxidation has been determined by cyclic voltammetry. Thermodynamic parameters for Ni−H and N−H bonds in important intermediates and the thermodynamic driving force for H_2 addition to the catalyst have also been determined. These data allow a detailed comparison with previously studied nickel diphosphine complexes and lead to conclusions regarding the optimum number of pendant bases required for high catalytic activity in these nickel systems. In addition, a further advance resulting from the study of these mixed-ligand complexes has been the identification of new intermediates that provide more detailed insight into the mechanism of H_2 addition to **3**. Spectroscopic studies have yielded quantitative data on the rates of intramolecular proton exchange between nickel and the proton relay within the cyclic ligand, and relative energies of relevant intermediates have been calculated. A detailed mechanism for the electrochemical oxidation of hydrogen catalyzed by nickel complexes containing proton relays in the second coordination sphere is presented.

Results

Syntheses of Mixed Ligand Complexes. 3, which contains one positioned pendant base, was synthesized by reacting stoichiometric amounts of the ligand $P^{Ph}_2N^{Bz}_2$ and 1,3-bis(diphenylphosphino)propane (dppp) with $[Ni(CH_3CN)_6](BF_4)_2$ in dry dichloromethane for 2 h. The red, moderately air-sensitive product was isolated by removal of solvent under vacuum. The ^{31}P NMR spectrum of $[Ni(dppp)(P^{Ph}_2N^{Bz}_2)](BF_4)_2$ exhibits two triplets, consistent with two different diphosphine ligands coordinated to nickel. These two resonances account for greater than 95% of the products by integration, with the impurities being the previously characterized symmetric complexes $[Ni(dppp)_2](BF_4)_2$[30] and $[Ni(P^{Ph}_2N^{Bz}_2)_2](BF_4)_2$.[21] Product **3** was not purified further because attempts at recrystallization were unsuccessful; slow evaporation or cooling of the reaction mixture resulted in preferential precipitation of the less-soluble complex $[Ni(P^{Ph}_2N^{Bz}_2)_2](BF_4)_2$. After about 24 h in coordinating solvents such as acetonitrile, a solution of $[Ni(dppp)(P^{Ph}_2N^{Bz}_2)](BF_4)_2$ decreases in purity to about 90% by integration of the ^{31}P NMR spectra, with a corresponding growth in the two symmetric compounds, $[Ni(P^{Ph}_2N^{Bz}_2)_2](BF_4)_2$ and $[Ni(dppp)_2](BF_4)_2$.

A second mixed ligand complex $[Ni(dppp)(P^{Ph}_2N^{Ph}_2)](BF_4)_2$ was synthesized in a similar procedure, isolated in pure form, and fully characterized. Data are included in the Experimental Section. However, selectivity for mixed-ligand derivatives of this class is not always observed. NMR scale reactions in CD_2Cl_2 of $[Ni(CH_3CN)_6](BF_4)_2$ with 1 equiv of $P^{Ph}_2N^{Ph}_2$ and 1 equiv of dmpm ($Me_2PCH_2PMe_2$), dppm ($Ph_2PCH_2PPh_2$), dppe ($Ph_2PCH_2CH_2PPh_2$), or dmpp ($Me_2P(CH_2)_3PMe_2$), which were monitored by ^{31}P NMR spectroscopy, all afforded mixtures of the homoleptic bis(diphosphine) complexes with the desired mixed-ligand complex present in yields ranging from 32% to 54% of soluble products.

The synthesis of the mixed-ligand Ni^0 complex, **4**, was first attempted using the precursor $Ni(COD)_2$. However, the sequential addition of the two ligands to $Ni(COD)_2$ resulted in the

(21) Fraze, K.; Wilson, A. D.; Appel, A. M.; Rakowski DuBois, M.; DuBois, D. L. *Organometallics* **2007**, *26*, 5003–5009.
(22) Wilson, A. D.; Fraze, K.; Twamley, B.; Miller, S.; DuBois, D. L.; Rakowski DuBois, M. *J. Am. Chem. Soc.* **2008**, *130*, 1061–1068.
(23) Henry, R. M.; Shoemaker, R. K.; Newell, R. H.; Jacobsen, G. M.; DuBois, D. L.; Rakowski DuBois, M. *Organometallics* **2005**, *24*, 2481–2491.
(24) Henry, R. M.; Shoemaker, R. K.; DuBois, D. L.; Rakowski DuBois, M. *J. Am. Chem. Soc.* **2006**, *128*, 3002–3010.
(25) Jacobsen, G. M.; Shoemaker, R. K.; Rakowski DuBois, M.; DuBois, D. L. *Organometallics* **2007**, *26*, 4964–4971.
(26) Jacobsen, G. M.; Shoemaker, R. K.; McNevin, M. J.; Rakowski DuBois, M.; DuBois, D. L. *Organometallics* **2007**, *26*, 5003.
(27) Jacobsen, G. M.; Yang, J. Y.; Twamley, B.; Wilson, A. D.; Bullock, R. M.; Rakowski DuBois, M.; DuBois, D. L. *Energy Environ. Sci.* **2008**, *1*, 167–174.
(28) Rakowski DuBois, M.; DuBois, D. L. C. R. *Chim.* **2008**, *11*, 805–817.
(29) Rakowski DuBois, M.; DuBois, D. L. *Chem. Soc. Rev.* **2009**, *38*, 62–72.
(30) Miedaner, A.; Haltiwanger, R. C.; DuBois, D. L. *Inorg. Chem.* **1991**, *30*, 417–427.

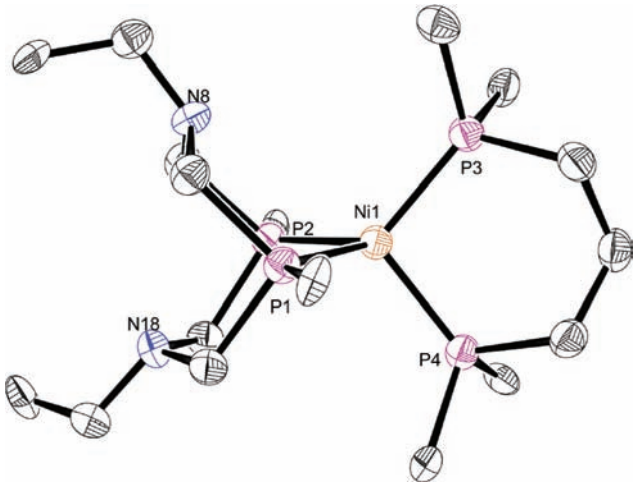

Figure 1. Structure of [Ni(dppp)($P^{Ph}_2N^{Bz}_2$)] (**4**) showing the atom numbering scheme. Thermal ellipsoids are shown at 80% probability level. Only ipso carbons of phenyl rings are shown.

Table 1. Selected Bond Distances (Å) and Angles (deg) for [Ni(dppp)($P^{Ph}_2N^{Bz}_2$)], **4**

bond distances		bond angles	
Ni(1)−P(1)	2.1238(8)	P(1)−Ni(1)−P(2)	85.63(3)
Ni(1)−P(2)	2.1397(7)	P(1)−Ni(1)−P(4)	108.97(3)
Ni(1)−P(4)	2.1401(8)	P(2)−Ni(1)−P(4)	118.87(3)
Ni(1)−P(3)	2.1502(8)	P(1)−Ni(1)−P(3)	117.00(3)
Ni(1)···N(8)	3.399	P(2)−Ni(1)−P(3)	124.19(3)
Ni(1)···N(18)	3.762	P(4)−Ni(1)−P(3)	101.66(3)

preferential formation of [Ni(dppp)$_2$] and [Ni($P^{Ph}_2N^{Bz}_2$)$_2$], as indicated by ^{31}P NMR spectroscopy. Fortunately, [Ni(dppp)($P^{Ph}_2N^{Bz}_2$)] could be successfully synthesized from **3** by bubbling hydrogen through an acetonitrile solution of **3**, followed by addition of excess triethylamine, reaction 1. The resulting neutral complex [Ni(dppp)($P^{Ph}_2N^{Bz}_2$)] precipitates as

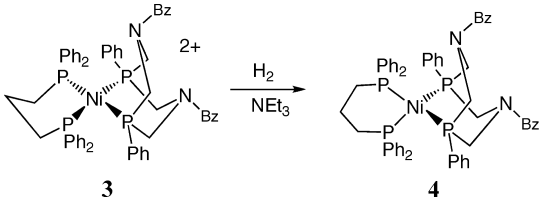

3 **4** (1)

an orange crystalline solid. This complex decomposes in dichloromethane and undergoes exchange of the diphosphine ligands in benzonitrile solution over a period of hours to form mixtures of [Ni(dppp)$_2$], [Ni($P^{Ph}_2N^{Bz}_2$)$_2$], and [Ni(dppp)($P^{Ph}_2N^{Bz}_2$)] (3:3:94 after 12 h). In contrast to **3**, for which two triplets were observed by ^{31}P NMR spectroscopy, **4** exhibits two singlets at 19.8 and 0.2 ppm in benzene-d_6. The observation of two equally intense resonances with decreased coupling compared to the Ni(II) analogue is consistent with a distorted tetrahedral complex in which the dihedral angle between the two diphosphine ligands is close to 90°.

This structural assignment for **4** was confirmed by a single-crystal X-ray diffraction study as shown in Figure 1. Selected bond distances and angles are given in Table 1. The complex is a distorted tetrahedron with all four Ni−P bond distances nearly equal at 2.12−2.15 Å. The P−Ni−P bond angles for the two diphosphine ligands are significantly different, 85.63° for $P^{Ph}_2N^{Bz}_2$ and 101.66°for dppp. Both are significantly less

Scheme 1

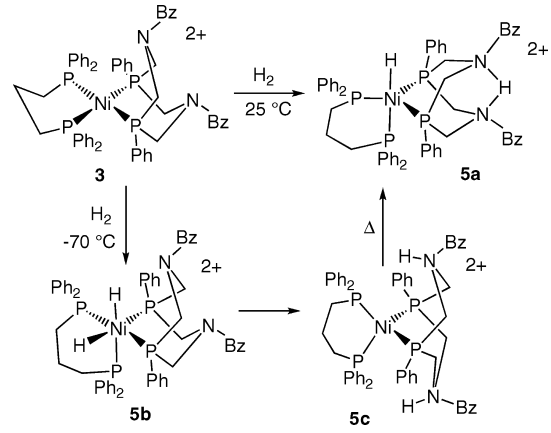

than the 109° expected for an ideal tetrahedron. The smaller bite angle observed for the $P^{Ph}_2N^{Bz}_2$ ligand compared to the dppp ligand is attributed to constraints imposed by the second six-membered chelate ring in the backbone of the cyclic ligand. The dppp ligand forms a six-membered ring in the chair form. $P^{Ph}_2N^{Bz}_2$ forms two such rings upon coordination; one is in the boat form, directing the pendant base toward the metal center (Ni−N distance = 3.40 Å) and the other is in the chair form (Ni−N distance = 3.76 Å). The dihedral angle between the two planes formed by the two phosphorus atoms of each diphosphine ligand and the Ni atom is 88°, close to the 90° angle expected for a tetrahedral complex.

Reaction of [Ni(dppp)($P^{Ph}_2N^{Bz}_2$)]$(BF_4)_2$ with Hydrogen at Room Temperature. 3 in acetonitrile or dichloromethane reacts rapidly upon addition of one atm of H_2 at room temperature to form a pale yellow solution of the product [HNi(dppp)($P^{Ph}_2N^{Bz}$(μ-H)N^{Bz})]$(BF_4)_2$, **5a**, according to the top reaction shown in Scheme 1. The addition of hydrogen displays some reversibility; purging the solution with nitrogen results in the reappearance of starting material, although the reverse reaction does not proceed cleanly. Repeated attempts to grow crystals of **5a** under an atmosphere of H_2 were unsuccessful. Both the ^{1}H and ^{2}H NMR spectra of **5a**, produced from H_2 and D_2, respectively, were investigated. At room temperature in CD_2Cl_2 no metal hydride resonance is observed. When the solution is cooled to −10 °C or lower, the hydride region of the ^{1}H NMR spectrum displays an overlapping triplet of triplets, consistent with a hydride ligand coupling to two nonequivalent diphosphine ligands (see top spectrum in Figure 2, solid trace). This pattern collapsed to a broad singlet at −8.9 ppm in the ^{31}P-decoupled ^{1}H NMR spectrum. In the corresponding ^{2}H NMR spectrum, the metal deuteride resonance is a broad singlet at −8.9 ppm, as seen in Figure 2 (top spectrum, dotted trace).

In this product of heterolytic H_2 cleavage, the nature of the protonated amine ligand was also established by multinuclear NMR experiments. The $P^{Ph}_2N^{Bz}_2$ ligand of **5a** can be protonated on a single amine, or the proton can bridge between both amines. The downfield resonance at 11.7 ppm in the ^{1}H (bottom of Figure 2, dotted trace) and ^{2}D NMR spectra suggests the latter.[19] To confirm this assignment, the ^{15}N-labeled analogue of **5a** was synthesized using $P^{Ph}_2{}^{15}N^{Bz}_2$ made from ^{15}N-labeled benzylamine. In the ^{1}H NMR spectrum of the ^{15}N-labeled complex, the peak corresponding to the protonated amine is a triplet with a coupling constant of 36.5 Hz, as seen in Figure 2 (lower spectrum, solid trace). This is consistent with a proton interacting with both amines, as depicted in **5a** of Scheme 1.

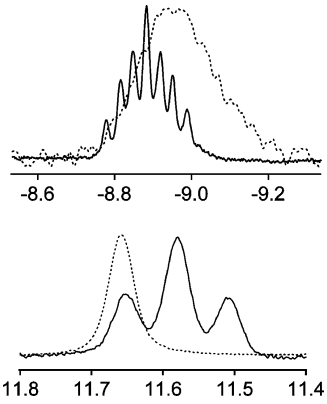

Figure 2. Top spectra are of the hydride resonance of **5a** of Scheme 1 which is formed by reaction of **3** with H_2 (^{1}H NMR, solid trace) or D_2 (^{2}D NMR, dotted trace). (b) Bottom spectra are of the N−H resonance observed upon addition of H_2 to ^{15}N-labeled **3** (solid trace) or the unlabeled compound (dotted trace) to form labeled and unlabeled **5a**, respectively. All spectra were recorded at −40 °C in CD_2Cl_2 on a 500 MHz spectrometer.

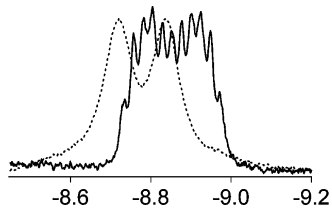

Figure 3. 500 MHz ^{1}H NMR (solid trace) and ^{1}H{^{31}P} NMR (dotted trace) spectra of the hydride resonance of intermediate $[(H)_2Ni(dppp)(P^{Ph}{}_2N^{Bz}{}_2)](BF_4)_2$, **5b**, formed upon reaction of $[Ni(dppp)(P^{Ph}{}_2N^{Bz}{}_2)](BF_4)_2$ with H_2 at −70 °C in CD_2Cl_2.

Reaction of $[Ni(dppp)(P^{Ph}{}_2N^{Bz}{}_2)](BF_4)_2$ with Hydrogen at Low Temperature. The structure of the H_2-addition product observed at room temperature, **5a**, suggests that rearrangement of the cyclic ligand is facile under these conditions. In order to identify intermediate species in H_2 or D_2 addition to **3**, the reaction was monitored at low temperature by ^{1}H, ^{2}H, and ^{31}P NMR spectroscopies. Hydrogen was bubbled through a dichloromethane-d_2 solution of **3** at −78 °C, and the ^{31}P and ^{1}H spectra were then recorded with the NMR probe cooled to −70 °C. At this temperature, the ^{31}P spectrum displays two AB patterns at 29.4 and 4.1 ppm (Figure S1 in the Supporting Information) that are tentatively assigned to a dihydride species, $[(H)_2Ni(dppp)(P^{Ph}{}_2N^{Bz}{}_2)](BF_4)_2$, **5b**, as shown in Scheme 1. The corresponding ^{1}H NMR spectrum at −70 °C displays a complex multiplet (11 line pattern) at −8.8 ppm (Figure 3, solid line). When the spectrum is ^{31}P decoupled (Figure 3, dotted line) this complex multiplet appears as two broad equally intense resonances assigned to inequivalent hydride ligands. To rule out the possibility that this is a dihydrogen complex, HD was used to synthesize this intermediate at low temperatures. The ^{1}H NMR spectrum indicated that hydrogen had substituted in both hydride positions, but the spectrum showed no evidence of HD coupling.

In the ^{31}P NMR spectrum at −70 °C, in addition to the dihydride species **5b**, a second complex, **5c**, is observed with two broad singlets at 19.4 and 9.7 ppm (Figure S1). The relative intensities of the resonances indicate that the ratio of **5b** to **5c** is roughly 1:1. These new resonances are attributed to the intermediate $[Ni(dppp)(P^{Ph}{}_2N^{Bz}{}_2H_2)](BF_4)_2$, a Ni^0 complex with two protonated N atoms, in which the N−H protons are endo with respect to nickel (**5c** of Scheme 1). This endo geometry is expected for a process proceeding through a dihydride complex followed by metal-to-nitrogen proton transfers to the pendant amines. In an effort to unambiguously confirm the formation of N−H bonds in **5c**, 2-dimensional ^{1}H−^{15}N NMR HSQC spectra were recorded at −70 °C on the product of the reaction of H_2 with ^{15}N-labeled $[Ni(dppp)(P^{Ph}{}_2N^{Bz}{}_2)](BF_4)_2$. A cross peak was observed for the ^{15}N resonance at 74.8 ppm and a proton resonance at 5.7 ppm, supporting the formation of an N−H bond at −70 °C. The chemical shift of the proton bound to nitrogen is in the region expected for a terminal N−H, as opposed to a bridging, N−H−N species.[20] In addition, the ^{31}P NMR chemical shift of the protonated ligand (9.7 ppm) is similar to that of this same protonated ligand for $[Ni(P^{Ph}{}_2N^{Bz}{}_2H)_2](BF_4)_2$ (9.6 ppm) which has previously been assigned[19,21] an endo structure. We were unable to detect a Ni−H (or Ni−D) resonance of **5c** by ^{1}H or ^{2}H NMR spectroscopy over a temperature range of −70 to 25 °C in CD_2Cl_2 that would be expected if heterolytic cleavage of H_2 to form N−H and Ni−H bonds occurred. In addition, the failure to observe phosphorus−phosphorus coupling for this species by ^{31}P NMR is more consistent with a Ni^0 complex than with a five-coordinate hydride complex, for which significant coupling would be expected, e.g., $J_{PP} = 40$ Hz for **5a**. These results are consistent with the addition of H_2 to $[Ni(dppp)(P^{Ph}{}_2N^{Bz}{}_2)](BF_4)_2$, **3**, at low temperature to form a dihydride complex (**5b**), followed by two rapid and reversible proton transfers to form $[Ni(dppp)(P^{Ph}{}_2N^{Bz}H_2)](BF_4)_2$, **5c**, and finally isomerization to **5a**, as shown in Scheme 1.

As the temperature is increased from −70 to −20 °C, the ^{31}P resonances of the dihydride **5b** and the endo complex **5c** significantly broaden (Figure S1), indicating exchange between the isomers at −20 °C at a rate calculated to be between 10^1 −10^2 s^{-1} using the ^{31}P NMR line widths. With further warming to 20 °C, the resonances for **5b** and **5c** disappear as the resonances assigned to **5a** increase. When the solution is recooled to −45 °C, only **5a** is present.

Variable-temperature NMR spectra performed in CD_3CN gave similar, but not identical results. At −45 °C, **3** reacts with H_2 (1.0 atm) to form a species exhibiting two singlets at 18.4 and 8.5 ppm in the ^{31}P spectrum, assigned to isomer **5c**. Only traces of the dihydride species **5b** are observed. Upon warming to room temperature **5c** converts to **5a**. However, in this case, recooling the sample to −45 °C results in formation of an ∼1:1 mixture of **5a** and **5c**. Although **5a** is favored in dichloromethane solution, the NMR data indicate that the endo and exo isomers have similar energies in acetonitrile.

Protonation of $[Ni(dppp)(P^{Ph}{}_2N^{Bz}{}_2)]$. Reaction of the Ni^0 complex, $[Ni(dppp)(N^{Ph}{}_2P^{Bz}{}_2)]$, with 1 equiv of anisidinium tetrafluoroborate ($pK_a = 11.9$ in acetonitrile)[31] results in the singly protonated complex, $[Ni(dppp)(P^{Ph}{}_2N^{Bz}HN^{Bz})](BF_4)$, **6**, as shown in step 1 of reaction 2, along with an equivalent of anisidine. The low temperature (−40 °C) ^{15}N NMR spectrum of ^{15}N-labeled **6** displays two unique resonances at 76.7 and 46.4 ppm. The former is consistent with a protonated amine, and the latter with an unprotonated amine, which suggests the proton is added to a single amine on the ligand, as opposed to being shared between the two, or located on the metal. The proposed structure is supported by the ^{31}P NMR spectrum, which displays one resonance for the $P^{Ph}{}_2N^{Bz}HN^{Bz}$ ligand (5.5 ppm),

(31) (a) Kaljurand, I.; Kutt, A.; Soovali, L.; Rodima, T.; Maemets, V.; Leito, I.; Koppel, I. A. *J. Org. Chem.* **2005**, *70*, 1019–1028. (b) Izutsu, K. *Acid-Base Dissociation Constants in Dipolar Aprotic Solvents, IUPAC Chemical Data Series, No. 35*; Blackwell Scientific Publications: Oxford, 1990.

and two inequivalent resonances for the dppp ligand (22.2 and 20.2 ppm) at −40 °C (Figure S2). The data are consistent with a tetrahedral coordination at Ni^0, which places one phosphorus atom of dppp in close proximity to the protonated amine. As the temperature is raised to room temperature, the two phosphorus resonances corresponding to dppp coalesce to form one peak, and an exchange rate of greater than 10^4 s^{-1} at 10 °C was determined from the ^{31}P NMR line widths. This exchange is also evident in the room temperature ^{15}N NMR spectrum, which displays only one resonance at 61.7 ppm, a chemical shift that is the average of those of the two resonances observed at low temperature. These results indicate that the proton of **6** is rapidly exchanging between the two amines on the NMR time scale at room temperature. This exchange could occur by either an intra- or intermolecular pathway, but the exchange rate suggests the former. At concentrations of 3 mM, a second-order rate constant of 10^9 M^{-1} s^{-2} would be required for an intermolecular process to give the observed exchange rate. Since this is near the diffusion-controlled limit, the reaction is most consistent with an intramolecular process. Upon recooling from 25 to −40 °C, the exchange can be slowed and then halted, giving rise to the low-temperature ^{31}P and ^{15}N spectra described above.

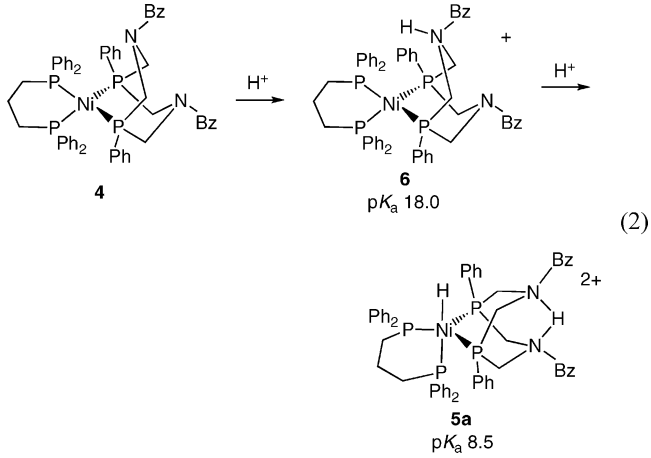

(2)

Another possibility for the equivalence of the two ^{15}N chemical shifts of $[Ni(dppp)(P^{Ph}{}_2N^{Bz}HN^{Bz})](BF_4)$, **6**, at room temperature is the formation of a $P^{Ph}{}_2N^{Bz}(\mu\text{-H})N^{Bz}$ ligand with a proton interacting with both amines as observed for **5a**. However, if this were true, a ^{15}N NMR chemical shift similar to that observed in **5a** (74.8 ppm) would be expected rather than the observed shift of 61.7 ppm. In addition, for a $P^{Ph}{}_2N^{Bz}(\mu\text{-H})N^{Bz}$ ligand, the ^{31}P NMR chemical shift is expected to be approximately the same as that for **5a** at room temperature (−9.7 ppm). Instead, the room temperature chemical shift (5.5 ppm) is nearly the same as the low-temperature chemical shift (5.2 ppm). The observed temperature dependence of **6** is therefore assigned to an exchange of a proton between the two N atoms to form equivalent endo geometries and not a temperature-dependent structural rearrangement to form an exo geometry. ^{31}P NMR spectroscopy confirms that addition of an equivalent of $HBF_4 \cdot OEt_2$ to **6** protonates the Ni atom to give the hydrogen addition product **5a**, as shown in step 2 of reaction 2.

Thermodynamic Data for Hydrogen Addition to $[Ni(dppp)(P^{Ph}{}_2N^{Bz}{}_2)](BF_4)_2$. To obtain thermodynamic information on the N−H bond in **6**, the weak acid $HNEt_3^+$ BF_4^- was added to **4** in benzonitrile (since **4** is not soluble in acetonitrile). Under these conditions equilibrium is observed for the first step of reaction 2. The ratios of **4** and **6** were determined using ^{31}P NMR spectroscopy, and the ratios of $HNEt_3^+$ BF_4^-/Et_3N were determined by mass balance. These data were used to calculate an equilibrium constant of 0.18 for step 1 of reaction 2. This equilibrium constant and a pK_a value of 18.8 for triethylammonium in acetonitrile[31] were used to determine a pK_a value of 18.0 ± 0.2 for **6**. (Previous studies have shown that relative pK_a values in acetonitrile and benzonitrile are the same within experimental error.)[32]

The pK_a value for **6**, along with the redox potentials of $[Ni(dppp)(P^{Ph}{}_2N^{Bz}{}_2)](BF_4)_2$, can be used to determine a hydride donor ability ($\Delta G°_{H^-}$) of 68.4 ± 2.0 kcal/mol for **6** using Scheme 2. Although it may seem somewhat nonintuitive to think of a hydride donor ability for the protonated amine in this complex, from a thermodynamic perspective, a hydride transfer reaction is equivalent to the transfer of a proton and two electrons from this protonated Ni^0 complex, generating a Ni^{II} complex. For comparison, the hydride donor ability of **6** is less than that of $[HNi(P^{Ph}{}_2N^{Bz}{}_2)](BF_4)$ (57.1 kcal/mol) but comparable to that of $[HNi(PNP)_2](BF_4)$ (66.7 kcal/mol) (where PNP = $Et_2PCH_2N(CH_3)CH_2PEt_2$).[18,21] A smaller $\Delta G°_{H^-}$ value represents a better hydride donor.

Addition of more than 1 equiv of the stronger acid *p*-trifluoroanilinium tetrafluoroborate in acetonitrile results in an equilibrium between **6** and **5a**, step 2 of reaction 2. Because the addition of H_2 to $[Ni(dppp)(P^{Ph}{}_2N^{Bz}{}_2)](BF_4)_2$ to form **5a** is slightly reversible, formation of this same product by addition of two protons to the Ni^0 derivative results in the liberation of some hydrogen to give $[Ni(dppp)(P^{Ph}{}_2N^{Bz}{}_2)](BF_4)_2$, complicating the equilibrium measurement. Performing the equilibrium measurements under a hydrogen atmosphere circumvented this problem. The ratio of **6** and **5a** was determined by ^{31}P NMR spectroscopy. The relative concentrations of the acid *p*-trifluoroanilinum and its conjugate base were determined from the resonances of the aromatic protons in the ^1H NMR spectrum. The chemical shifts of these resonances are a weighted average of the values for the respective pure acid and base because of rapid exchange on the NMR time scale. Using these data, an equilibrium constant of 3.2 was determined for step 2 of reaction 2 at 22 °C. This equilibrium constant and a pK_a value of 8.0

Scheme 2

Determining the Hydride Donor Ability of $[Ni(dppp)(P^{Ph}{}_2N^{Bz}HN^{Bz})](BF_4)$, 6

$[Ni(dppp)(P^{Ph}{}_2N^{Bz}HN^{Bz})]^+ \rightarrow [Ni(dppp)(P^{Ph}{}_2N^{Bz}{}_2)] + H^+$ $\quad \Delta G° = 1.37(pK_{a1}) = 24.7$ kcal/mol

$[Ni(dppp)(P^{Ph}{}_2N^{Bz}{}_2)] \rightarrow [Ni(dppp)(P^{Ph}{}_2N^{Bz}{}_2)]^{2+} + 2\ e^-$ $\quad \Delta G° = 46.1E°(II/0) = -35.9$ kcal/mol

$H^+ + 2\ e^- \rightarrow H^-$ $\quad \Delta G° = 46.1E°(H^+/H^-) = 79.6$ kcal/mol

$[Ni(dppp)(P^{Ph}{}_2N^{Bz}HN^{Bz})]^+ \rightarrow [Ni(dppp)(P^{Ph}{}_2N^{Bz}{}_2)]^{2+} + H^-$ $\quad \Delta G°_{H^-} = 68.4$ kcal/mol

Scheme 3

Determining the Free Energy of H_2 addition to $[Ni(dppp)(P^{Ph}{}_2N^{Bz}{}_2)](BF_4)_2$, 3.

$$[Ni(dppp)(P^{Ph}{}_2N^{Bz}{}_2)]^{2+} + H^- \rightarrow [Ni(dppp)(P^{Ph}{}_2N^{Bz}HN^{Bz})]^+ \qquad \Delta G^\circ_{H^-} = -68.4 \text{ kcal/mol}$$

$$[Ni(dppp)(P^{Ph}{}_2N^{Bz}HN^{Bz})]^+ + H^+ \rightarrow [HNi(dppp)(P^{Ph}{}_2N^{Bz}(\mu\text{-}H)N^{Bz})]^{2+} \qquad \Delta G^\circ = -1.37(pK_{a2}) = -11.6 \text{ kcal/mol}$$

$$H_2 \rightarrow H^+ + H^- \qquad \Delta G^\circ = 76 \text{ kcal/mol}$$

$$[Ni(dppp)(P^{Ph}{}_2N^{Bz}{}_2)]^{2+} + H_2 \rightarrow [HNi(dppp)(P^{Ph}{}_2N^{Bz}(\mu\text{-}H)N^{Bz})]^{2+} \qquad \Delta G^\circ_{H_2} = -4.0 \text{ kcal/mol}$$

for *p*-trifluoroanilinium in acetonitrile[31] were used to calculate a pK_a of 8.5 for the Ni−hydride ligand in **5a**. A pK_a value of 8.4 was determined for **5a** using the acid *p*-bromoanilinium tetrafluoroborate (pK_a = 9.4),[31] providing a crosscheck of the values obtained using this method.

On the basis of a $\Delta G^\circ_{H^-}$ value of 68.4 kcal/mol for **6** and a pK_a value of 8.5 for the hydride ligand of **5a**, the free energy associated with the addition of hydrogen to form **5a** can be determined using the thermodynamic cycle shown in Scheme 3. The ΔG° of H_2 addition is calculated to be −4.0 kcal/mol. This value is consistent with the slight reversibility of the H_2 addition reaction that was observed experimentally.

Electrochemical Studies. The cyclic voltammogram of **3** recorded in acetonitrile displays two reversible reduction waves at −0.52 and at −1.04 V vs the ferrocenium/ferrocene couple (ΔE_p = 70 and 67 mV, respectively at a scan rate of 100 mV/s). These are assigned to the $Ni^{II/I}$ and $Ni^{I/0}$ couples, respectively. Plots of i_p versus the square root of the scan rate are linear for both waves, indicating that both electron-transfer events are diffusion-controlled (Figures S3 and S4 of Supporting Information). The corresponding cyclic voltammogram of the Ni^0 complex, **4**, recorded in benzonitrile (**4** is insoluble in acetonitrile) consists of two reversible one-electron oxidation waves (ΔE_p = 68 mV at a scan rate of 100 mV/s) at −1.07 and −0.53 V vs the ferrocenium/ferrocene couple (shown in black in Figure 4), very close to the numbers recorded in acetonitrile for **3**. The $Ni^{I/0}$ couple measured for **3** at −1.04 V is nearly the average (−1.05 V) for those of $Ni(dppp)_2$ (−0.91 V)[30] and $[Ni(P^{Ph}{}_2N^{Bz}{}_2)_2]$ (−1.19 V). Similarly, the $Ni^{II/I}$ couple for **3** of −0.52 V lies midway between that of $Ni(dppp)_2$ (−0.12 V in dichloromethane) and $[Ni(P^{Ph}{}_2N^{Bz}{}_2)_2]$ (−0.94 V).

Figure 4 also displays the cyclic voltammograms of **4** recorded in benzonitrile purged with hydrogen (red trace), and upon addition of 1.5 equiv of triethylamine (blue trace). Without any base present (red trace), **4** does not react with hydrogen until it is oxidized to the Ni^{2+} complex (**3**), upon which the oxidation wave at −0.53 V is enhanced. Two new reduction waves are observed with peaks at −0.80 and −1.46 V, respectively, which are attributed to the hydrogen adduct **5**. Cyclic voltammograms in which only the $Ni^{I/0}$ couple is traversed indicate that this wave is unchanged and still fully reversible in the presence of hydrogen. Addition of NEt_3 to give a 3 mM solution (1.5 equiv relative to catalyst) results in essentially no increase in the anodic current observed for the wave at −0.53 V (blue scan). Higher concentrations of triethylamine did not result in any further increase in current. In the presence of triethylamine, the waves assigned to the H_2 adduct are not observed, consistent with a fast deprotonation of the H_2 adduct to form **4**. The oxidative current for the $Ni^{II/I}$ couple in the presence of H_2 plus triethylamine is approximately a factor of 2.3 larger than the current observed for the $Ni^{II/I}$ couple in the absence of H_2 and base. A simple ECE mechanism with no catalysis would result in a similar current enhancement. However, the plateau shape of the wave indicates a slow catalytic reaction with a catalytic rate of 0.5 s^{-1} or less.[18]

To obtain further information on the rate of H_2 addition to the electrochemically generated $[Ni(dppp)(P^{Ph}{}_2N^{Bz}{}_2)](BF_4)_2$, a scan rate dependence study of $[Ni(dppp)(P^{Ph}{}_2N^{Bz}{}_2)]$ in the presence of 1.0 atm of H_2 was performed, and the results are shown in Figure 5. As the scan rate increases, the waves associated with the H_2 adduct decrease, and the two reduction waves associated with $[Ni(dppp)(P^{Ph}{}_2N^{Bz}{}_2)](BF_4)_2$ increase. By comparing the ratios of the peak current of the reduction or cathodic wave (i_c) for the $Ni^{I/0}$ couple to the peak current observed for the oxidation or anodic wave (i_a) for this same couple as a function of the time between the oxidation and reduction waves (Figure 6), it can be determined that 50% of $[Ni(dppp)(P^{Ph}{}_2N^{Bz}{}_2)](BF_4)_2$ is converted to the H_2 adduct, **5**, in 1.8 s, for a rate of addition of 0.4 s^{-1} under these conditions. The study was also carried out under 1 atm of deuterium gas. A similar analysis determined that 50% of

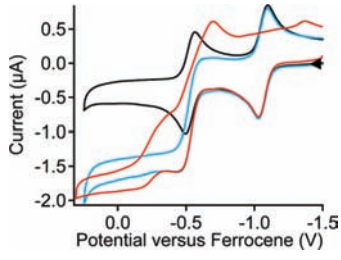

Figure 4. Cyclic voltammogram of a 2.0 mM solution of **4** under nitrogen (black), under hydrogen (red), and in 3.0 mM Et_3N under hydrogen (blue). Conditions: scan rate = 100 mV/s, benzonitrile solvent, 0.2 M Bu_4NBF_4 as supporting electrolyte, glassy carbon working electrode. Potentials are referenced to the ferrocenium/ferrocene couple.

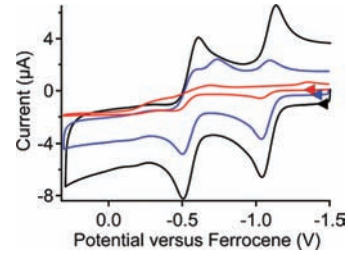

Figure 5. Cyclic voltammogram of a 1.5 mM solution of $[Ni(dppp)(P^{Ph}{}_2N^{Bz}{}_2)]$ under 1.0 atm of hydrogen using a scan rate of 50 mV/s (red), 1.0 V/s (blue), and 3.0 V/s (black). Conditions: benzonitrile solvent, 0.2 M Bu_4NBF_4 as supporting electrolyte, glassy carbon working electrode. Potentials are referenced to the ferrocenium/ferrocene couple.

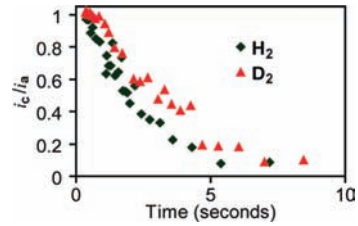

Figure 6. Plot of the ratio of the cathodic peak current to the anodic peak current (i_c/i_a) for the $Ni^{I/0}$ couple of **4** as a function of time for the wave at −1.07 V in the presence of 1.0 atm of H_2 (black diamonds) and 1.0 atm of D_2 (red triangles).

$[Ni(dppp)(P^{Ph}{}_2N^{Bz}{}_2)](BF_4)_2$ had reacted with D_2 after 3.0 s. This gives a kinetic isotope effect of 1.7 for the oxidation of H_2.

Discussion

Proposed Mechanism for Electrocatalytic Oxidation of Hydrogen. Hydrogen Cleavage. The electrochemical and spectroscopic studies indicate that **3** is a catalyst for H_2 oxidation, although the rate is slow (0.4 s^{-1} at 1.0 atm of H_2) with a kinetic isotope effect of 1.7. Previous studies of electrocatalytic H_2 oxidation by $[Ni(diphosphine)_2](BF_4)_2$ complexes containing pendant bases have shown that the rate-limiting step is the addition of H_2 to the Ni^{II} complex.[18−21] However, neither dihydride or dihydrogen intermediates have been detected experimentally in previous systems. The spectroscopic studies of the reaction of $[Ni(dppp)(N^{Ph}{}_2P^{Bz}{}_2)](BF_4)_2$ with H_2 provide the first experimental data for the existence of a Ni^{IV} dihydride intermediate in the catalytic cycle and provide a more detailed mechanistic picture of the catalytic cycle than was possible in earlier studies. A proposed cycle is shown in Scheme 4. For clarity, the substituents on phosphorus and nitrogen are not shown.

The initial H_2 addition step is thought to involve the reversible formation of an undetected dihydrogen complex (step A), which has been implicated by theoretical studies for both $[Ni(PNP)_2](BF_4)_2$ and $[Ni(P^{Cy}{}_2N^{Bz}{}_2)_2](BF_4)_2$.[20] This dihydrogen species undergoes a rate-determining H−H bond scission to form the corresponding dihydride complex as shown in step B, for which spectroscopic evidence has now been obtained. It is suggested that step A represents a preequilibrium, and step B, the oxidative addition of H_2, is the overall rate-determining step in the catalytic cycle. The turnover frequency of 0.4 s^{-1} under 1 atm H_2 is determined by the equilibrium constant associated with step A and the rate constant for step B. Our observed isotope effect of 1.7 for the addition of H_2 to **3** is consistent with previously reported values of equilibrium and kinetic isotope effects. Equilibrium isotope effects for binding of $H_2(D_2)$ to metals are typically inverse ($K_{H_2}/K_{D_2} \approx 0.4-0.7$)[33] though they can be normal at some temperatures.[34] Kinetic isotope effects (k_{H_2}/k_{D_2}) for oxidative addition of H_2 (D_2) to metals are typically between 1 and 2.[33] Our observed isotope effect is a composite influenced by both the equilibrium isotope effect for H_2 (D_2) binding and the kinetic isotope effect for oxidative addition of H_2 (D_2). As a result the individual values are not determined by our experiments.

Because the rate-determining step in the catalytic oxidation of H_2 is the cleavage of hydrogen, we are interested in understanding both the thermodynamic and kinetic factors controlling this reaction in greater detail. The free energy associated with H_2 addition to **3** is −4.0 kcal/mol. This value is compared to those reported for the other nickel diphosphine systems with pendant amines in Table 2. The $\Delta G^o_{H_2}$ for **3** is significantly more favorable than the $\Delta G^o_{H_2} = +2.7$ kcal/mol found for $[Ni(P^{Ph}{}_2N^{Bz}{}_2)_2]^{2+}$; this correlates with an increase in the hydride acceptor ability of **3** of 11 kcal/mol. The increased driving force for H_2 addition to the mixed ligand complex is attributed to the greater tetrahedral distortion of the complex that results from the much larger bite angle of the dppp ligand relative to that of $P^{Ph}{}_2N^{Bz}{}_2$. In an extensive series of $[Ni(diphosphine)_2]^{2+}$ derivatives, greater tetrahedral distortions have been shown to lead to a decrease in the energy of the lowest

Scheme 4[a]

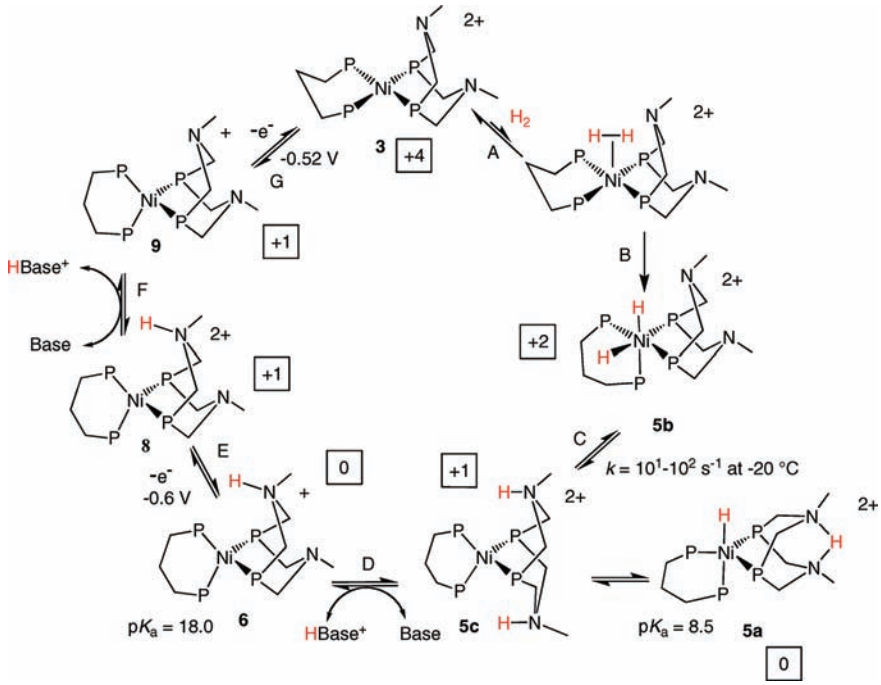

[a] Relative free energies are shown in the squares in kcal/mol (1.0 atm of H_2, pH 8.5).

Table 2. Thermodynamic Properties and Turnover Frequencies of $[Ni(diphosphine)_2](BF_4)_2$ Complexes with Pendant Amines

complex	$\Delta G°_{H^-}$ kcal/mol	pK_a NH	$\Delta G°_{(H_2)}$ kcal/mol	turnover frequency $(s^{-1})^a$
$[Ni(P^{Ph}_2N^{Bz}_2)_2](BF_4)_2$[21]	57.1	11.8	+2.7	[b]
$[Ni(P^{Cy}_2N^{Bz}_2)_2](BF_4)_2$[21]	60.7	13.4	−3.1	10
$[Ni(dppp)(N^{Ph}_2P^{Bz}_2)](BF_4)_2$	68.4	8.5[c]	−4.0	0.4
$[Ni(PNP)_2](BF_4)_2$[18]	66.7	11.2	−6.0	<0.2

[a] Turnover frequency for oxidation of H_2 under 1.0 atm of H_2 at 22 °C. [b] This complex catalyzes the formation of H_2 by reduction of H^+. [c] pK_a of hydride ligand of **5a**.

unoccupied molecular orbital resulting from a decrease in the sigma antibonding interaction between nickel and phosphorus. This lower energy enhances the hydride acceptor abilities for the Ni^{II} complexes[30,35] and also favors oxidative addition of H_2.[36]

The data in Table 2 illustrate that in the series of electrocatalysts for oxidation of H_2, the thermodynamic driving force for the addition of H_2 increases in the order: $[Ni(P^{Cy}_2N^{Bz})_2](BF_4)_2$ < **3** < $[Ni(PNP)_2](BF_4)_2$.[18,19,21] However, the turnover frequencies, which are correlated with the *rates* of H_2 addition, show the reverse order. These rates correlate with the *number of positioned amines in the second coordination sphere of each complex* (not the total number of pendant amines). These comparisons strongly support the premise that *two positioned* pendant bases are important for achieving the fast catalytic rates observed for $[Ni(P^{Cy}_2N^{Bz}_2)_2](BF_4)_2$ in the oxidation of H_2, and for $[Ni(P^{Ph}_2N^{Ph}_2)_2](BF_4)_2$ in the production of H_2. The role of the two amines positioned in close proximity to the metal serves to stabilize, through hydrogen bonding interactions, both the binding of the dihydrogen ligand on nickel and the symmetrical heterolytic cleavage of H_2. This role appears to be particularly important for nickel systems, for which other discrete dihydrogen or Ni^{IV} dihydride complexes are to the best of our knowledge unknown. In contrast, the cobalt complex, $[Co(P^{Ph}_2N^{Ph}_2)(CH_3CN)_3](BF_4)_2$, does not display the same structural requirements for high catalytic activity.[27] Although this complex contains only one positioned pendant amine base, it has been found to be a very active electrocatalyst for H_2 production.[27] Nevertheless, the significantly higher activity observed for nickel complexes containing two positioned bases compared to those without this structural feature provides a valuable criterion for developing future nickel-based catalysts for H_2 oxidation and production.

Proton and Electron Transfer Steps. Although the cleavage of H_2 in steps A and B of Scheme 4 determines the overall catalytic rate of H_2 oxidation, the proton-transfer steps (C, D, and F) and electron-transfer steps (E and G) are important in determining the overpotential of the catalytic reaction. In this system all of the intermediates involved in these steps are nearly isoenergetic (1.0 atm of H_2, pH 8.5), avoiding high- or low-energy species, and the relative energies (in kcal/mol) for intermediate species are included in Scheme 4 as shown by the numbers in boxes. For example, step C in Scheme 4 involves the rapid reversible transfer of two protons from Ni to the N atoms of the cyclic ligand to form isomer **5c**. Our spectroscopic data indicate that this process is fast, 10−100 s^{-1} at −20 °C, and reversible. In dichloromethane-d_2, the concentrations of **5b** and **5c** are nearly equal at low temperatures (Figure S1), consistent with nearly equal energies. In acetonitrile **5c** is the dominant species (**5c**/**5b** ratio ≈ 10:1). Complex **5c** converts slowly to **5a**, and the free energy for formation of **5a** from **3** and H_2 at 1.0 atm is −4.0 kcal/mol. This data has been used to calculate the relative free energies of **5b**, **5c**, and **5a**, shown in the scheme and discussed in more detail in the Supporting Information. The nearly equal energies of **5b**, **5c**, and **5a** and the rapid interconversion of **5b** and **5c** illustrate that transfer of one or even two protons between the ligand and nickel is energetically and kinetically facile.

Step D in the catalytic cycle (Scheme 4) is the deprotonation of **5c** to form **6**. The pK_a of **5a** was determined to be 8.5, and therefore at pH of 8.5, **5a** and **6** are of equal energy (both at 0 kcal/mol as indicated in Scheme 4). The addition of a single equivalent of a weak acid to **4** provides an alternate pathway to the monoprotonated nickel complex **6**, which has been characterized by NMR spectroscopy. It was initially surprising that the site of addition for the first proton is the amine in the cyclic ligand and not the Ni^0 center as observed for $[Ni(PNP)_2]$ and $[Ni(P^{Cy}_2N^{Bz}_2)_2]$,[18,19] but the assigned structure with a protonated amine is supported by the appropriate chemical shifts of two resonances in the ^{15}N NMR spectrum, as well as other spectroscopic data.

The pK_a of the protonated amine of **6** in acetonitrile was found to be 18.0. It is interesting to compare this value with the pK_a estimated for the Ni^{II} complex, $[HNi(dppp)(P^{Ph}_2N^{Bz}_2)](BF_4)$, **7**, an unobserved isomer of the Ni^0 complex, **6**, in which the proton has transferred from nitrogen to nickel. A pK_a value of 17.6 ± 1.5 can be calculated for **7** from the potential of the $Ni^{I/0}$ couple of **4** (−1.04 V) using linear free energy relationships described previously (equation 3).[21,37] The difference in the observed pK_a value for **6** and the calculated pK_a value for **7** (0.4 pK_a units) suggests that isomer **7** and **6** have nearly equal energies, but since **7** is not observed experimentally, it is likely to be 2−3 kcal/mol higher in energy than **6**. The observation of a rapid exchange of a proton between the two amine sites of **6** (greater than 10^4 s^{-1} above 10 °C) is proposed to involve an intramolecular proton transfer from N to Ni followed by a second proton transfer from Ni to the second N atom. A fast transfer of a proton between the pendant endo nitrogen atom of the ligand and nickel is consistent with isomers **6** and **7** being nearly isoenergetic.

$$pK_a = -20.8 \times E_{1/2}^{(I/0)} - 4.0 \qquad (3)$$

Step E in the catalytic cycle is the oxidation of **6** to form **8**, an N-protonated Ni^I complex. Equation 3 allows us to estimate that the potential for the $Ni^{I/0}$ couple of **6** is −0.6 V (see Supporting Information for details). This step is followed by a very fast proton transfer to a base in solution to form the Ni^I complex, $[Ni(dppp)(N^{Ph}_2P^{Bz}_2)](BF_4)$ (**9**) (step F), which is oxidized to Ni^{II} (**3**) (step G) to complete the cycle for the catalytic oxidation of H_2. This final oxidation occurs at −0.52 V, a potential slightly more positive than that for step E, and it is therefore the potential required for the overall catalytic cycle.

(32) Berning, D.; Noll, B.; DuBois, D. L. *J. Am. Chem. Soc.* **1999**, *121*, 11432–11447.
(33) Bullock, R. M.; Bender, B. R. Isotope Methods -Homogeneous. In *Encyclopedia of Catalysis*; Horváth, I. , Ed.; Wiley: New York, 2002, Vol. 4, pp 281−348.
(34) Parkin, G. *Acc. Chem. Res.* **2009**, *42*, 315–325.
(35) Raebiger, J. W.; Miedaner, A.; Curtis, C. J.; Miller, S. M.; DuBois, D. L. *J. Am. Chem. Soc.* **2004**, *126*, 5502–5514.
(36) DuBois, D. L.; Blake, D. M.; Miedaner, A.; Curtis, C. J.; DuBois, M. R.; Franz, J. A.; Linehan, J. C. *Organometallics* **2006**, *25*, 4414–4419.
(37) Berning, D.; Miedaner, A.; Curtis, C. J.; Noll, B. C.; Rakowski DuBois, M.; DuBois, D. L. *Organometallics* **2001**, *20*, 1832–1839.

In our previous studies of the electrocatalytic oxidation of H_2 by $[Ni(PNP)_2](BF_4)$ and $[Ni(P^{Cy}{}_2N^{Bz}{}_2)_2](BF_4)_2$, the oxidation potentials of the hydride complexes $[HNi(PNP)_2](BF_4)$ and $[HNi(P^{Cy}{}_2N^{Bz}{}_2)_2](BF_4)_2$ occur at potentials 0.5−0.6 V negative of those observed or expected for analogues with no pendant base. These large shifts in potential indicate that a proton-coupled electron transfer (PCET) process is occurring. Previous studies of PCET in various systems have proposed sequential proton- and electron-transfer processes (in either order) or concerted processes.[38−42] In our previous reports on the nickel complexes we suggested that the intermediate Ni^{II} hydride species listed above were oxidized to Ni^{III} hydrides and then deprotonated.[18,20,28] In the present system, the corresponding species is **6**, formally a Ni^0 complex, in which the proton is bound to a nitrogen atom instead of nickel. The observation of this species has allowed us to estimate for the first time that the difference in energy between protonated amine and nickel-hydride species such as **6** and **7** is likely less than 3 kcal/mol, as discussed above. This suggests that proton transfer from nickel to nitrogen may also be very facile for the previously studied systems, and the sequences in the respective catalytic cycles involving $[HNi(PNP)_2](BF_4)$ and $[HNi(P^{Cy}{}_2N^{Bz})_2](BF_4)$ may proceed via a proton transfer from nickel to nitrogen followed by electron transfer from the N-protonated Ni^0 complexes. If this is true, then the electron transfer events involve $Ni^{I/0}$ couples rather than $Ni^{III/II}$ couples. This pathway avoids high-energy Ni^{III} hydrides that are inherent in the direct oxidation of nickel hydride complexes without proton relays.[18]

Summary

The Ni^{II} and Ni^0 complexes, $[Ni(dppp)(P^{Ph}{}_2N^{Bz}{}_2)](BF_4)_2$ and $[Ni(dppp)(P^{Ph}{}_2N^{Bz}{}_2)]$, containing a single positioned pendant base are reported. The Ni^{II} complex is an electrocatalyst for H_2 oxidation. The rate of the overall catalytic cycle is determined by a preequilibrium involving the reversible formation of a dihydrogen adduct followed by the cleavage of the H−H bond to form a dihydride complex. Using low-temperature NMR studies, the formation of the dihydride intermediate has been observed spectroscopically for the first time in these catalytic systems. This complex evolves to form a species containing Ni−H and N−H bonds at room temperature, resulting in the overall heterolytic cleavage of H_2. Thermodynamic studies reported here indicate that intramolecular proton-transfer reactions between nickel and nitrogen are associated with free energy changes less than 3 kcal/mol, and the rates of intramolecular proton exchange between nickel and nitrogen are fast ($>10^3$ s^{-1} at room temperature). The similar energies observed for the Ni^0 complex, **6**, and the Ni^{II} hydride, **7**, suggest that proton-coupled electron-transfer reactions in all of the nickel diphosphine catalysts containing pendant bases are likely to proceed by initial transfer of a proton from nickel to the pendant base of the diphosphine ligand, followed by electron transfer. The close energy matching of the pK_a values of the protonated amine ligands and the corresponding nickel hydride isomers provides new low-energy pathways for catalysis that avoid the large overpotentials associated with Ni^{III} hydride intermediates.

Although the free energy of H_2 addition to $[Ni(dppp)(P^{Ph}{}_2N^{Bz}{}_2)](BF_4)_2$ is more favorable than that for H_2 addition to $[Ni(P^{Cy}{}_2N^{Bz}{}_2)_2](BF_4)_2$, the rate of H_2 oxidation by the latter complex is ∼20 times faster. This higher catalytic activity is attributed to the cooperative participation of *two positioned* pendant bases which are important for stabilizing the dihydrogen intermediate shown in structure **1**, as well as the dihydride intermediate resulting from H−H bond cleavage. Both the number and positioning of pendant bases play an important role in the design of molecular catalysts, and in these nickel diphosphine systems, the positioning of two pendant bases is critical for high catalytic activity for H_2 oxidation and production.

Experimental Section

General Experimental Procedures. ^1H, ^2H, ^{15}N, and ^{31}P NMR spectra were recorded on a Varian Inova spectrometer (500 MHz for ^1H) at 20 °C unless otherwise noted. All ^1H chemical shifts have been internally calibrated to the monoprotio impurity of the deuterated solvent. The ^2H NMR spectra were internally calibrated to the monodeutero impurity in the undeuterated solvent used. The ^{31}P NMR spectra were proton decoupled and referenced to external phosphoric acid. The ^{15}N NMR spectra were proton decoupled and referenced to an aqueous $^{15}NH_4Cl$ solution.

All electrochemical experiments were carried out under an atmosphere of nitrogen, or hydrogen when indicated, in 0.2 M Et_4NBF_4 acetonitrile solutions or 0.2 M Bu_4NBF_4 benzonitrile solutions. Cyclic voltammetry experiments were performed with a CH Instruments model 660C potentiostat. Ferrocene was used as an internal standard, and all potentials are referenced to the ferrocenium/ferrocene couple. Electrospray ionization (ESI) mass spectra were collected using an HP 5989B mass spectrometer with a HP 59987A electrospray.

Synthesis and Materials. All reactions and manipulations were performed under an N_2 atmosphere using standard Schlenk techniques or a glovebox unless otherwise indicated. Solvents were dried using an activated alumnia column. $[Ni(CH_3CN)_6](BF_4)_2$,[43] $P^{Ph}{}_2N^{Bz}{}_2$,[21] and $[Ni(P^{Ph}{}_2N^{Bz}{}_2)_2](BF_4)_2$[21] were prepared using literature methods. The ^{15}N-labeled $P^{Ph}{}_2N^{Bz}{}_2$ was prepared analogously to the unlabeled ligand.

$[Ni(dppp)(P^{Ph}{}_2N^{Ph}{}_2)](BF_4)_2$. A mixture of $[Ni(CH_3CN)_6](BF_4)_2$ (0.100 g, 0.20 mmol), 1,3-bis(diphenylphosphino)propane (0.083 g, 0.20 mmol), and $P^{Ph}{}_2N^{Ph}{}_2$ (0.091 g, 0.20 mmol) in dichloromethane (30 mL) was stirred at room temperature for 0.75 h to form a dark red solution. The solvent was removed under vacuum (0.140 g, 64% yield). Anal. Calcd for $C_{55}H_{54}P_4N_2B_2F_8Ni$: C, 60.10; H, 4.95; N, 2.54. Found: C, 59.68; H, 4.71; N, 2.41. ^1H NMR (CD_2Cl_2): 7.58−7.00 (m, PC_6H_5); 4.50 (d, PCH_2N); 3.87 (d, PCH_2N); 2.23 (m, $PCH_2CH_2CH_2$); 1.81 ppm (m, $PCH_2CH_2CH_2$). ^{31}P NMR (CD_2Cl_2): 4.95 (m, $P^{Ph}{}_2N^{Ph}{}_2$); 1.01 ppm (m, dppp). ESI^+ (CH_3OH): *m/z* 1011 $\{[(Ni(dppp)(P^{Ph}{}_2N^{Ph}{}_2)](BF_4)\}^+$; *m/z* 462 $\{[(Ni(dppp)(P^{Ph}{}_2N^{Ph}{}_2)]\}^{2+}$. CV ($Bu_4NPF_6$ in CH_2Cl_2): $E_{1/2}$ or E_p if irreversible, V vs ferrocene (ΔE_p, mV) = −0.41 (100); −0.98 (85). Oxidations: 0.96 (irrev).

$[Ni(dppp)(P^{Ph}{}_2N^{Bz}{}_2)](BF_4)_2$, 3. Diphenylphosphinopropane (dppp) (0.412 g, 1.0 mmol) and $P^{Ph}{}_2N^{Bz}{}_2$ (0.482 g, 1.0 mmol) were dissolved in 40 mL of dichloromethane. $[Ni(CH_3CN)_6](BF_4)_2$ (0.500 g, 1.0 mmol) was added, and the solution was stirred at room temperature for 3 h. The solvent was then removed under vacuum to leave a dark red solid that was not purified further. The ^{15}N-labeled compound was synthesized in the same fashion using the ^{15}N-labeled ligand $P^{Ph}{}_2N^{Bz}{}_2$. ^1H NMR (CD_3CN): 7.72−7.06 (m, 40H), 4.00 (s, 4H), 3.43 (m, 4H), 3.20 (m, 4H), 2.60 (s, 4H), 1.13 ppm (br s, 2H). ^{31}P NMR (CD_3CN): 6.66 (t, $P^{Ph}{}_2N^{Bz}{}_2$, J_{PP} = 75 Hz), −2.30 ppm (t, dppp).

(38) Rhile, I. J.; Markle, T. F.; Nagao, H.; DiPasquale, A. G.; Lam, O. P.; Lockwood, M. A.; Rotter, K.; Mayer, J. M. *J. Am. Chem. Soc.* **2006**, *128*, 6075–6088.
(39) Cukier, R. I.; Nocera, D. G. *Annu. Rev. Phys. Chem.* **1998**, *49*, 337–369.
(40) Mayer, J. M. *Annu. Rev. Phys. Chem.* **2004**, *55*, 363–390.
(41) Costentin, C. *Chem. Rev.* **2008**, *108*, 2145–2179.
(42) Huynh, M. H. V.; Meyer, T. J. *Chem. Rev.* **2007**, *107*, 5004–5064.
(43) Heintz, R. A.; Smith, J. A.; Szalay, P. S.; Weisgerber, A.; Dunbar, K. R. *Inorg. Syn.* **2002**, *33*, 72.

Table 3. Crystal Data and Structure Refinement for **4**

empirical formula	$C_{59}H_{61}N_3NiP_4$	
formula weight	994.70	
temperature	90(2) K	
wavelength	0.71073 Å	
crystal system	monoclinic	
space group	$P2_1/c$	
unit cell dimensions	$a = 18.3808(7)$ Å	$\alpha = 90°$
	$b = 11.6486(4)$ Å	$\beta = 97.353(1)°$
	$c = 23.6805(9)$ Å	$\gamma = 90°$
volume	5028.5(3) Å^3	
Z	4	
density (calculated)	1.314 Mg/m^3	
absorption coefficient	0.556 mm^{-1}	
$F(000)$	2096	
crystal size	0.27 × 0.07 × 0.04 mm^3	
crystal color and habit	orange needle	
diffractometer	Bruker/Siemens SMART APEX	
θ range for data collection	1.73−25.25°	
index ranges	$-22 \le h \le 22$,	
	$-13 \le k \le 13$,	
	$-28 \le l \le 28$	
reflections collected	74 657	
independent reflections	9108 [R(int) = 0.0796]	
completeness to $\theta = 25.25°$	100.0%	
Absorption correction	semiempirical from equivalents	
max. and min. transmission	0.9781 and 0.8645	
solution method	XS, SHELXTL v. 6.14 (Bruker, 2003)	
refinement method	full-matrix least-squares on F^2	
data/restraints/parameters	9108/0/605	
goodness-of-fit on F^2	1.013	
final R indices [$I > 2\sigma(I)$]	R1 = 0.0406, wR2 = 0.0886	
R indices (all data)	R1 = 0.0655, wR2 = 0.0999	
largest diff. peak and hole	0.645 and −0.266 e Å^{-3}	

[Ni(dppp)($P^{Ph}_2N^{Bz}_2$)], 4. 3 (0.300 g, 0.260 mmol) was dissolved with $P^{Ph}_2N^{Bz}_2$ (10 mg, 0.021 mmol) in 6.0 mL of acetonitrile. Hydrogen gas was bubbled through the solution for about 15 min followed by addition of 100 μL of triethylamine (0.721 mmol). After standing about 24 h, orange crystals precipitated. The crystals were isolated by filtration and washed with 2 × 2 mL aliquots of acetonitrile (0.15 g, 60% yield). X-ray quality crystals were grown using the same procedure on a smaller scale. ^{1}H NMR (C_6D_6): 7.62−6.96 (m, 40H), 3.45 (s, 4H), 3.07 (d, J = 11 Hz, 4H), 2.61 (d, J = 11 Hz, 4H), 2.33 (s, 4H), 1.7 ppm (bs, 2H). ^{31}P NMR (C_6D_6): 19.77 (s, dppp), 0.18 ppm (s, $P^{Ph}_2N^{Bz}_2$). Anal. Calcd for $C_{57}H_{58}N_2NiP_4$: C, 71.79; H, 6.13; N, 2.94. Found: C, 72.27; H, 6.22; N, 2.92.

Reactions of 3 with Hydrogen to form [HNi(dppp)($P^{Ph}_2N^{Bz}$(μ-H)N^{Bz})](BF_4)$_2$, 5a. In NMR tube experiments, a solution of **3** in CD_2Cl_2 or CD_3CN was purged with hydrogen and the reaction was followed by ^{1}H and ^{31}P NMR spectroscopy. This was performed at room temperature. Variable-temperature NMR spectra of the H_2 addition products were obtained by purging solutions of **3** with H_2 in a dry ice/acetone bath, followed by insertion into the precooled spectrometer probe. The formation of **5** can be followed by a color change from red to yellow, and this reaction is complete within 1 min at room temperature. ^{31}P{^{1}H} NMR (CD_2Cl_2): 15.94 (t, J = 40 Hz, dppp), −9.73 ppm (br s, $P^{Ph}_2N^{Bz}_2$). ^{31}P{^{1}H} NMR (CD_3CN): 16.69 (t, J = 44 Hz, dppp), −11.63 ppm (t, J = 44 Hz, $P^{Ph}_2N^{Bz}_2$). ^{1}H NMR (CD_2Cl_2, −40 °C): 11.7 (N-*H*-N, br s), −8.6 ppm (Ni-*H*, tt, $^2J_{PH}$ = 20, 35 Hz). With ^{15}N-labeled compound, ^{1}H NMR (CD_2Cl_2, T = −40 °C): 11.6 ppm (^{15}N-*H*-^{15}N, t, J = 36.5 Hz). Using D_2, ^{2}H NMR (CD_2Cl_2, T = −40 °C): 11.8 (N-*D*-N, br s), −8.9 ppm (Ni-*H*, br s).

Reaction of 4 with 1 equiv of *p*-Anisidinium Tetrafluoroborate to Form [Ni(dppp)($P^{Ph}_2N^{Bz}HN^{Bz}$)](BF_4)·ansidine, 6. *p*-Anisidinium tetrafluoroborate (15 mg, 0.043 mmol) was added to a solution of **4** (41 mg, 0.043 mmol) in 5 mL of benzene. After 1 h at room temperature, the reaction solution was filtered, and the solvent was removed from the yellow-orange filtrate to leave a solid product (40 mg, 97% yield). The ^{15}N-labeled compound was synthesized in the same fashion using the ^{15}N-labeled ligand $P^{Ph}_2N^{Bz}_2$. ^{31}P NMR (benzonitrile): 19.20 (t, dppp), 5.45 ppm (t, $P^{Ph}_2N^{Bz}_2$), observed splitting = 7 Hz; (acetone-d_6): T = 20 °C, δ 20.50 (s), 5.51 (s); T = −40 °C, δ 22.15(s), 20.17 (s), 5.24 (s). ^{15}N NMR (acetone-d_6): T = 20 °C, δ 61.7; T = −40 °C, δ 76.7, 46.4.

pK_a Determination of 6. In a representative procedure, 0.5 mL of a 1.0 mM benzonitrile solution of **4** was added to a NMR tube followed by a 100 μL aliquot of a 25 mM benzonitrile solution of triethylammnonium tetrafluoroborate (5 equiv), and the tube was shaken. After 10 min, the sample was analyzed by ^{31}P NMR to determine the ratio of the reactant and the product. The ^{31}P NMR spectrum showed two resonances matching those of the reactant **4**, and two matching those of complex **6**, which was independently synthesized as described above. The NMR was rerecorded 1 h later to ensure the system was at equilibrium, and the same ratio was observed within experimental error. The procedure was repeated using aliquots of acid corresponding to 10, 20, 30, and 40 equiv to determine an equilibrium constant (K_1 = [**6**] × [NEt_3]/[**4**] × [$HNEt_3^+$]) of 0.18 ± 0.03. This equilibrium constant and the pK_a value of $HNEt_3BF_4$ in acetonitrile (18.8) was used to calculate a pK_a value for **6** of 18.0 ± 0.2.

pK_a Determination of 5a. In a representative procedure, 0.5 mL of a 0.01 M acetonitrile solution of **4** was added to an NMR tube. A 15 μL aliquot of a 0.38 M solution of 4-(trifluoromethyl)anilinium tetrafluoroborate (1.15 equiv) was added and the solution was shaken and purged with hydrogen. After 10 min, the sample was analyzed by ^{1}H and ^{31}P NMR. The ^{31}P NMR spectrum was used to determine the ratio of [Ni(dppp)($P^{Ph}_2HN^{Bz}_2$)](BF_4), **6**, and **5a**, each of which has two resonances. The ratios of 4-(trifluoromethyl)anilinium to 4-(trifluoromethyl)aniline were determined from the chemical shift of the aromatic resonances of the ^{1}H NMR spectra. Because of rapid proton exchange between the base and its protonated form at room temperature, the chemical shift of the resonance is a weighted average of the shifts of the protonated base (7.38, 6.73 ppm) and the free base (7.87, 7.60 ppm). The ^{1}H and

^{31}P NMR spectra were recorded 1 h later, and the same ratio was observed within experimental error. The procedure was repeated adding 20, 25, 30, and 35 μL of acid solution, and the results from all five samples were averaged to give an equilibrium constant (K_2 = [**5a**] × [$CF_3C_6H_4NH_2$]/[**6**] × [$CF_3C_6H_4NH_3^+$]) of 3.28 ± 0.13. This equilibrium constant and the pK_a value of $CF_3C_6H_4NH_3BF_4$ in acetonitrile (8.0) was used to calculate pK_a value for **5a** of 8.5 ± 0.2. As a cross-check, the same general procedure was used to determine a pK_a value of 8.4 using 4-bromoaniliniuim tetrafluoroborate (pK_a = 9.4 in acetonitrile).

Electrocatalytic Oxidation of Hydrogen with 4. A benzonitrile solution (2.5 mL) containing 0.2 M Bu_4NBF_4 and **4** (1.3 mM) was added to an electrochemical cell under nitrogen. After the solution was purged with hydrogen for 10 min, successive cyclic voltammograms were recorded upon addition of increasing amounts of triethylamine. The initial amount added was 0.5 μL (1.2 equiv) and the final amount was 50.0 μL (116 equiv). A plot of the plateau current versus equivalents of NEt_3 showed no dependence on base after addition of 1.2 equiv.

X-Ray Diffraction Studies. Crystals of compound **4** were removed from the flask, a suitable crystal was selected and attached to a glass fiber, and data were collected at 90(2) K using a Bruker/Siemens SMART APEX instrument (Mo Kα radiation, λ = 0.71073 Å) equipped with a Cryocool NeverIce low temperature device. Data were measured using omega scans 0.3°/frame for 30 s, and a full sphere of data was collected. A total of 2400 frames were collected with a final resolution of 0.77 Å. Cell parameters were retrieved using SMART[44] software and refined using SAINTPlus[45] on all observed reflections. Data reduction and correction for Lp and decay were performed using the SAINTPlus software. Absorption corrections were applied using SADABS.[46] The structure was solved by direct methods and refined by least-squares method on F^2 using the SHELXTL program package.[47] The structure was solved in the space group $P2_1/c$ (no. 14) by analysis of systematic absences. All non-hydrogen atoms were refined anisotropically. No decomposition was observed during data collection. Details of the data collection and refinement are given in Table 3. Further details are provided in the Supporting Information.

Acknowledgment. This work was supported by the Chemical Sciences program of the Office of Basic Energy Sciences of the Department of Energy. The Pacific Northwest National Laboratory is operated by Battelle for the U.S. Department of Energy. The Bruker (Siemens) SMART APEX diffraction facility was established at the University of Idaho with the assistance of the NSF-EPSCoR program and the M. J. Murdock Charitable Trust, Vancouver, WA.

Supporting Information Available: Crystallographic data for complex **4** in cif format, variable-temperature ^{31}P NMR spectra for compounds **5a**−**c** and **6**, and thermodynamic calculations. This material is available free of charge via the Internet at http://pubs.acs.org.

JA900483X

(44) *SMART, v. 5.632*; Bruker AXS: Madison, WI, 2005.
(45) *SAINTPlus, v. 7.23a: Data Reduction and Correction Program*; Bruker AXS: Madison, WI, 2004.
(46) *SADABS, v.2004/1: an empirical absorption correction program*; Bruker AXS Inc.: Madison, WI, 2004.
(47) Sheldrick, G. M. *SHELXTL, v. 6.14: Structure Determination Software Suite*; Bruker AXS Inc.: Madison, WI, 2004.